Inorganic Chemistry

Article

pubs.acs.org/IC

Field-Induced Single-Ion Magnets Based on Enantiopure Chiral β-Diketonate Ligands

Cai-Ming Liu,* De-Qing Zhang, and Dao-Ben Zhu

Beijing National Laboratory for Molecular Sciences, Center for Molecular Science, Institute of Chemistry, Key Laboratory of Organic Solids, Chinese Academy of Sciences, Zhongguancun Beiyijie No. 2, Beijing 100190, P. R. China

Supporting Information

ABSTRACT: A pair of homochiral β-diketonate ligands (+)-3-trifluoroacetyl)camphor (*d*-Htfc) and (−)-3-trifluoroacetyl)camphor (*l*-Htfc) were used to construct two enantiomeric pairs of Dy(III) single-ion magnets $[Dy(d\text{-tfc})_3(bpy)]_2$ (*d*-**1**)/$[Dy(l\text{-tfc})_3(bpy)]_2$ (*l*-**1**) (bpy = 2,2′-bipyridine) and $[Dy(d\text{-tfc})_3(phen)]\cdot 2H_2O$ (*d*-**2**)/$[Dy(l\text{-tfc})_3(phen)]$ (*l*-**2**) (phen = 1,10-phenanthroline). The capping aromatic *N*,*N*′-donors have a dramatic influence on the structural and magnetic characteristics of the Dy(III) β-diketonate enantiomeric pairs: the cocrystal of two homochiral Dy(III) β-diketonate stereoisomers with the 2,2′-bipyridine ligand was formed, showing field-induced single-ion magnet behaviors with a two-step relaxation process, while no stereoisomerization happened for the homochiral Dy(III) β-diketonate with the 1,10-phenanthroline coligand, exhibiting a single relaxation process of the magnetization only. The anisotropy barriers of *d*-**1** (36.5 and 46.1 K) are slightly smaller than those of *l*-**1** (37.0 and 49.3 K), while *d*-**2** has a larger energy barrier (30.5 K) with respect to *l*-**2** (25.1 K).

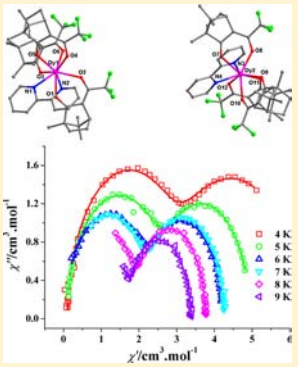

INTRODUCTION

Recently, it has become a practical strategy for assembly of multifunctional molecular materials utilizing enantiopure chiral isomers of organic ligands to transfer chiral information into the entire magnetic system through coordination bonds. The motivation is that chirality may bring extra functions such as the magnetochiral dichroism (MChD) effect,[1] second harmonic generation (SHG),[2] and ferroelectric properties[3] in magnetic molecules.[4] On the other hand, during the past two decades, much attention has been paid to the design and construction of single-molecule magnets (SMMs), which are characterized as slow magnetization relaxation caused by the association of large spin ground states (*S*) with a negative uniaxial magnetic anisotropy (*D*). The SMMs have found potential applications in high-density information storage, quantum information processing, and spintronics at the molecular level.[5] Furthermore, although most SMMs are polynuclear metallic complexes, recent research indicated that the assembly of SMMs utilizing a single ion is also feasible in lanthanide complexes,[6] actinide complexes,[7] Fe(III) complexes,[8] Fe(II) complexes,[9] and Co(II) complexes.[10] The magnetic anisotropy in these single-ion magnets (SIMs) has roots in the interaction between the single metal ion and the ligand field, leading to a preferential orientation of the magnetic moment,[7a] so the coordination geometry has a strong influence on the SIM properties. However, despite many endeavors, only limited success has been obtained due to the great challenge in synthesis of enantiopure chiral SMMs and SIMs,[11] with most chiral aggregates being apt to crystallize as racemic mixtures or encounter rapid racemization in solution.[3g]

It is well-known that β-diketonates are good bidentate chelating ligands, providing feasible ligand fields to investigate the SMMs/SIMs properties of simple lanthanide complexes. We are especially interested in the homochiral Dy(III) β-diketonate complexes with suitable capping ligands because some of them exhibit not only SMM/SIM properties but also other additional properties related to the chirality.[11a,d,f] Up to now, the chiral information of the reported homochiral Dy(III) β-diketonate SMMs/SIMs is just transferred from the chiral capping ligands.[11a,d,f] Considering the chirality is also able to come from the chiral β-diketonates themselves, we chose (+)/(−)-3-trifluoroacetyl)camphor (*d*-Htfc/*l*-Htfc, Scheme 1) as the enantiopure chiral ligands and applied 2, 2′-bipyridine (bpy) and 1,10-phenanthroline (phen) as the capping ligands to construct two new Dy(III) β-diketonate enantiomeric pairs, $[Dy(d\text{-tfc})_3(bpy)]_2$ (*d*-**1**)/$[Dy(l\text{-tfc})_3(bpy)]_2$ (*l*-**1**) and $[Dy(d\text{-tfc})_3(phen)]\cdot 2H_2O$ (*d*-**2**)/$[Dy(l\text{-tfc})_3(phen)]$ (*l*-**2**). Very intriguingly, two stereoisomers of the homochiral Dy(III) β-

Scheme 1. Enantiomeric Ligands (+)-3-Trifluoroacetyl)camphor (*d*-Htfc) and (−)-3-Trifluoroacetyl)camphor (*l*-Htfc)

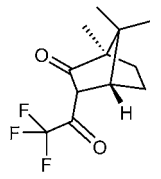

(+)-3-Trifluoroacetyl-camphor

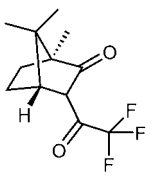

(-)-3-Trifluoroacetyl-L-camphor

Received: May 5, 2013
Published: July 16, 2013

   dx.doi.org/10.1021/ic4011218 | *Inorg. Chem.* 2013, 52, 8933−8940

Table 1. Crystal Data and Structural Refinement Parameters

	d-**1**	*l*-**1**	*d*-**2**	*l*-**2**
chemical formula	$C_{46}H_{50}DyF_9N_2O_6$	$C_{46}H_{50}DyF_9N_2O_6$	$C_{48}H_{54}DyF_9N_2O_8$	$C_{48}H_{50}DyF_9N_2O_6$
fw	1060.38	1060.38	1120.43	1084.40
cryst syst	triclinic	triclinic	orthorhombic	orthorhombic
space group	*P*1	*P*1	$P2_12_12_1$	$P2_12_12_1$
a/Å	12.267(2)	12.267(2)	10.903(2)	11.081(2)
b/Å	12.899(3)	12.899(3)	15.216(3)	14.459(3)
c/Å	16.729(3)	16.729(3)	29.672(6)	29.774(6)
α/deg	69.88(3)	69.88(3)	90.00	90.00
β/deg	73.43(3)	73.43(3)	90.00	90.00
γ/deg	71.44(3)	71.44(3)	90.00	90.00
V/Å^3	2309.9(8)	2309.9(8)	4922.6(17)	4770.4(16)
Z	2	2	4	4
T/K	173 (2)	173 (2)	173 (2)	173 (2)
λ(Mo K*α*)/Å	0.71073	0.71073	0.71073	0.71073
ρ_{calc}/g cm^{-3}	1.525	1.525	1.512	1.510
μ(Mo K*α*)/mm^{-1}	1.702	1.702	1.605	1.650
θ range	$2.00° \le \theta \le 25.00°$	$2.16° \le \theta \le 25.00°$	$1.99° \le \theta \le 26.36°$	$2.29° \le \theta \le 25.00°$
limiting indices	$-14 \le h \le 14, -15 \le k \le 15, -19 \le l \le 19$	$-14 \le h \le 14, -15 \le k \le 15, -19 \le l \le 19$	$-13 \le h \le 13, -18 \le k \le 16, -36 \le l \le 37$	$-13 \le h \le 13, -17 \le k \le 13, -29 \le l \le 35$
reflns collected	25 068	25 523	30 546	28 542
unique reflns	15 271	15 282	9967	8396
R1[a] [$I > 2\sigma(I)$]	0.0552	0.0490	0.0642	0.0595
wR2[b] [$I > 2\sigma(I)$]	0.1159	0.0956	0.1584	0.1352
R1[a] (all data)	0.0584	0.0522	0.0671	0.0695
wR2[b] (all data)	0.1195	0.0983	0.1610	0.1451
S	1.064	1.069	1.078	1.133

[a] $R1 = \sum||F_o| - |F_c||/\sum|F_o|$. [b] $wR2 = \sum\{[w(F_o^2 - F_c^2)^2]/\sum[wF_o^2]^2\}^{1/2}$.

diketonate complexes coexist in *d*-**1** (or *l*-**1**) as a cocrystal, displaying two magnetic relaxation processes. This work represents the first cocrystal of two stereoisomers of the homochiral lanthanide SIMs/SMMs. *d*-**1** and *l*-**1** are also the first examples where the two magnetic relaxation processes are associated with two cocrystallized stereoisomers rather than two different paramagnetic components of the same molecule or two crystallographically independent Dy^{3+} sites in the crystal structure.

EXPERIMENTAL SECTION

Materials and Characterization Techniques. All commercial chemicals were used as received without further purification. Elemental analyses were carried out on a Varlo ELIII elemental analyzer. IR spectra were recorded using a TENSOR27 Bruker spectrophotometer as KBr pallet in the range 4000−400 cm^{-1}. The CD spectra were recorded on a JASCO J-815 spectropolarimeter at room temperature. The magnetic susceptibility measurements were carried out on 'polycrystalline samples (7.28 mg of *d*-**1**, 7.92 mg of *l*-**1**, 7.05 mg of *d*-**2** and 8.88 mg of *l*-**2**) with a Quantum Design MPMS-XL5 SQUID magnetometer. Diamagnetic corrections were estimated from Pascal's constants for all constituent atoms.

Preparation of d-1. A mixture of (+)-3-trifluoroacetyl)camphor (*d*-tfc) (0.3 mmol) and Me_4NOH (10% aqueous solution) (0.3 mmol) in 40 mL of CH_3OH/MeCN (v/v 1:1) was stirred for 30 min at room temperature, and then 0.1 mmol of $DyCl_3$ and 0.1 mmol of 2,2′-bipyridine (bpy) were added in succession. After being stirred for another 24 h at room temperature, the resultant light-yellow solution was evaporated for 2 weeks, and light-yellow plate crystals of *d*-**1** were obtained (yield 55% based on Dy). Anal. Calcd for $C_{92}H_{100}Dy_2F_{18}N_4O_{12}$: C, 52.10; H, 5.23; N, 2.64%. Found: C, 52.03; H, 5.28; N, 2.59%. IR (KBr, cm^{-1}): 2962(m), 2874(w), 1653(s), 1602(w), 1577(w), 1546(m), 1477(w), 1439(m), 1390(w), 1375(w), 1331(m), 1297(w), 1269(m), 1228(s), 1201(m), 1185(m), 1130(s), 1080(w), 1054(w), 1010(w), 921(w), 805(w), 765(m), 740(w), 715(w), 682(w), 646(w), 557(w), 493(w), 416(w).

Preparation of l-1. Complex *l*-**1** was obtained as pale-yellow crystals by a method similar to that of *d*-**1**, except that (−)-3-trifluoroacetyl)camphor (*l*-tfc) was employed instead of (+)-3-trifluoroacetyl)camphor(*d*-tfc). Yield: 60% (based on Dy). Anal. Calcd for $C_{92}H_{100}Dy_2F_{18}N_4O_{12}$: C, 52.10; H, 5.23; N, 2.64%. Found: C, 52.13; H, 5.27; N, 2.60%. IR (KBr, cm^{-1}): 2961(m), 2874(w), 1653(s), 1602(w), 1577(w), 1545(m), 1477(w), 1439(m), 1390(w), 1375(w), 1331(m), 1297(w), 1269(m), 1228(s), 1202(m), 1186(m), 1130(s), 1080(w), 1054(w), 1011(w), 921(w), 805(w), 765(m), 740(w), 715(w), 683(w), 646(w), 557(w), 494(w), 417(w).

Preparation of d-2. A mixture of (+)-3-trifluoroacetyl)camphor (*d*-tfc) (0.3 mmol) and Me_4NOH (10% aqueous solution) (0.3 mmol) in 40 mL of CH_3OH/MeCN (v/v 1:1) was stirred for 30 min at room temperature, and then 0.1 mmol of $DyCl_3$ and 0.1 mmol of 1,10-phenanthroline (phen) were added in succession. After being stirred for another 24 h at room temperature, the resultant light-yellow solution was evaporated for 2 weeks, and light-yellow plate crystals of *d*-**2** were obtained (yield 50% based on Dy). Anal. Calcd for $C_{48}H_{50}DyF_9N_2O_6$: C, 53.16; H, 4.65; N, 2.58%. Found: C, 53.22; H, 4.71; N, 2.54%. IR (KBr, cm^{-1}): 3431(b, w), 3073(w), 2962(m), 2930(w), 2875(w), 1652(s), 1546(s), 1522(m), 1477(w), 1428(m), 1390(w), 1375(w), 1331(m), 1296(m), 1268(s), 1227(s), 1202(s), 1185(m), 1131(s), 1108(m), 1080(m), 1054(m), 1005(w), 921(w), 849(w), 804(w), 732(m), 682(w), 645(w), 557(w), 494(w), 415(w).

Preparation of l-2. Complex *l*-**2** was obtained as yellow crystals by a method similar to that of *d*-**2**, except that (−)-3-trifluoroacetyl)-camphor (*l*-tfc) was employed instead of (+)-3-trifluoroacetyl)-camphor (*d*-tfc). Yield: 55% (based on Dy). Anal. Calcd for $C_{48}H_{54}DyF_9N_2O_8$: C, 53.16; H, 4.65; N, 2.58%. Found: C, 53.11; H,

dx.doi.org/10.1021/ic4011218 | Inorg. Chem. 2013, 52, 8933−8940

4.71; N, 2.55%. IR (KBr, cm^{-1}): 2962(m), 2930(w), 2874(w), 1653(s), 1546(m), 1522(m), 1477(w), 1428(m), 1389(w), 1375(w), 1331(m), 1296(w), 1268(s), 1227(s), 1202(s), 1185(m), 1132(s), 1108(m), 1080(w), 1055(w), 1005(w), 921(w), 849(w), 804(w), 732(w), 682(w), 645(w), 557(w), 494(w), 416(w).

X-ray Crystallography. The diffraction data were collected with Mo Kα (λ = 0.710 73 Å) radiation using a Rigaku Saturn 724 diffractometer at 173(2) K. The data were corrected for Lorentz polarization effects, and absorption corrections were applied. The structures were solved by direct methods and refined with full-matrix least-squares techniques using *SHELXS*-97 and *SHELXL*-97 programs. All non-hydrogen atoms were refined anisotropically, and all hydrogen atoms were allowed for as riding atoms. Selected crystallographic data and structure determination parameters are given in Table 1. CCDC 929734−929737 contain the supplementary crystallographic data for this paper. These data can be obtained free of charge from The Cambridge Crystallographic Data Centre via www.ccdc.cam.ac.uk/data_request/cif.

RESULTS AND DISCUSSION

Preparation, Circular Dichroism (CD) Spectra, and Ferroelectric Studies. Reaction of (+)/(−)-3-trifluoroacetyl)camphor, $DyCl_3$ and 2,2′-bipyridine in the presence of Me_4NOH (10% aqueous solution) in CH_3OH/MeCN solution led to the formation of pale-yellow crystals of *d*-**1** and *l*-**1**, respectively. When the capping ligand 1,10-phenanthroline instead of 2,2′-bipyridine was used, pale-yellow crystals of *d*-**2** and *l*-**2**, respectively, were obtained. The optical activity and enantiomeric nature of *d*-**1**/*l*-**1** and *d*-**2**/*l*-**2** were verified by their circular dichroism (CD) spectra (Figure 1). In methanol solution, the spectrum of *d*-**1** shows a positive Cotton effect at λ_{max} = 241 and 306 nm, while *l*-**1** exhibits Cotton effects of the opposite sign at the same wavelengths. The typically positive and negative CD couplets around 306 nm are arising from the $\pi-\pi^*$ transition of the β-diketone ligands,[12] whereas the Cotton effects centered at 241 nm are assigned to the $\pi-\pi^*$ transition of the bpy ligands. The CD signals of the two compounds form an obvious mirror image, indicating that the *d*-**1** and *l*-**1** isomers are enantiomeric compounds. A similar trend was observed for the *d*-**2**/*l*-**2** compounds: *d*-**2** exhibits positive Cotton effects at λ_{max} = 240 and 304 nm, which originate from the $\pi-\pi^*$ transition of the β-diketone ligand and the phen ligand, respectively, and *l*-**1** shows Cotton effects with opposite signs at the same wavelengths. Although *d*-**1** and *l*-**1** crystallize in a polar point group (*P*1) required for ferroelectric properties, no ferroelectric behaviors were observed at room temperature for both complexes.

Crystal Structures. X-ray crystallographic analyses further confirmed that both *d*-**1**/*l*-**1** and *d*-**2**/*l*-**2** are pairs of enantiomers, which crystallize in the chiral space groups *P*1 and $P2_12_12_1$, respectively. Since the enantiomers possess similar structures, only the crystal structures of *d*-**1** and *d*-**2** are described in detail here. The most striking feature of *d*-**1** is that two homochiral stereoisomers are cocrystallized together (Figure 2); such a case is rather rare for the lanthanide complexes. In stereoisomer 1, all three *d*-tfc$^-$ asymmetric ligands are *cis* arranged and coordinated to the Dy1 ion, with their trifluoroacetyl groups being situated at the same side; however, in stereoisomer 2, only two trifluoroacetyl groups of the *d*-tfc$^-$ anions bound to the Dy2 ion are located at the same side, and the third trifluoroacetyl group of the *d*-tfc$^-$ ligand is situated at the other side. Therefore, it can be regarded that the third *d*-tfc$^-$ ligand results in two types of stereoisomers with two different bonding ways, with its trifluoroacetyl group *cis* or *trans* to the other two *cis* trifluoroacetyl groups of the *d*-tfc$^-$ ligands.

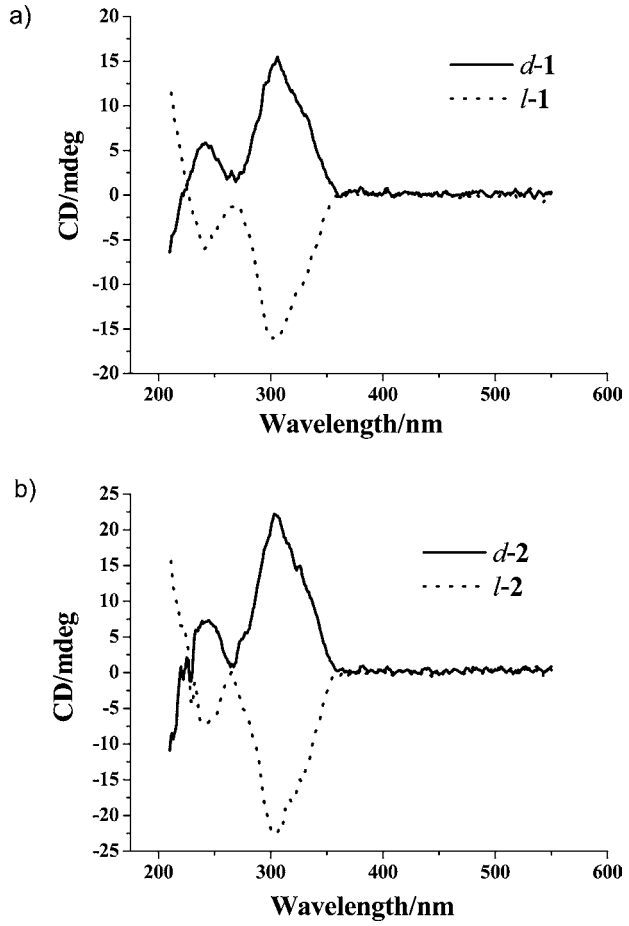

Figure 1. CD spectra of *d*-**1**/*l*-**1** (a) and *d*-**2**/*l*-**2** (b) at room temperature (2×10^{-5} M, MeOH).

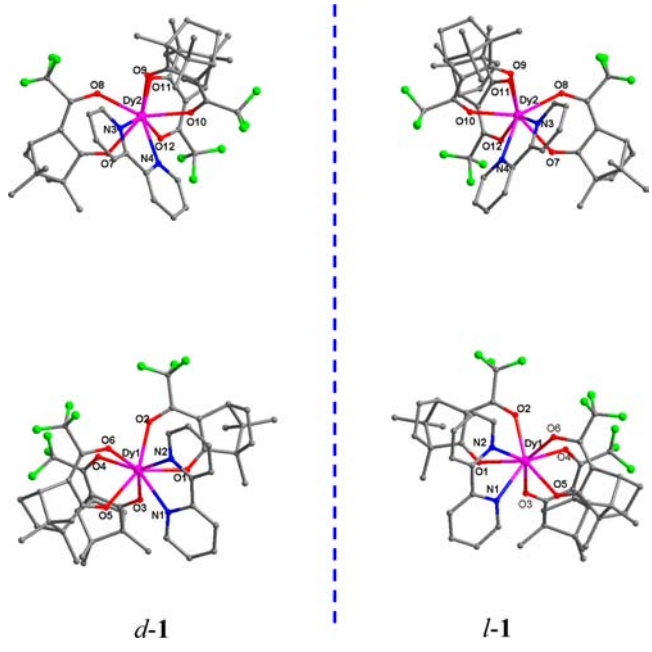

Figure 2. Enantiomeric pair of *d*-**1** and *l*-**1**, and all H atoms are omitted for clarity.

dx.doi.org/10.1021/ic4011218 | Inorg. Chem. 2013, 52, 8933−8940

The Dy^{3+} center of each stereoisomer is eight coordinated, completed by six O atoms from three *d*-tfc$^-$ ligands and two N atoms of the bpy ligand, generating a DyN_2O_6 coordination polyhedron (Figure S1, see the Supporting Information). A detailed analysis of coordination geometry by the creased angles of two approximate square planes is generally used to judge the eight-coordinate polyhedron conformations: the corresponding angles are 0° and 0° for a square antiprism, 29.5° and 29.5° for a dodecahedron, and 21.8° and 0° for a bicapped trigonalprism.[13] For the Dy1 atom of *d*-**1**, the two approximate square planes defined by O1−O2−O4−O3 and N1−N2−O6−O5 are creased about the respective diagonals O2−O3 and N2−O5 with angles of 10.3° and 6.7°. For the Dy2 atom, the creased angles of two approximate square faces defined by O7−O8−O11−O12 and O9−O10−N4−N3 about the respective diagonals O7−O11 and N3−O10 are 0.9° and 7.0°. Therefore, the polyhedron defined by the Dy^{3+} ion and its bound atoms can be best described as a distorted square antiprism geometry, and the square antiprism polyhedron of the Dy1 atom is more distorted than that of the Dy2 atom. As shown in Table 2, both the N−Dy1−N bond angle (63.2°) and the O−Dy1−O bond angle defined by the *d*-tfc$^-$ ligand and the Dy1 atom (mean value of 74.85°) in stereoisomer 1 are slightly larger than the corresponding N−Dy2−N bond angle (63.0°) and O−Dy2−O bond angle (mean value of 74.38°) in stereoisomer 2. The Dy1−N bond distances (2.553 and 2.554 Å) in stereoisomer 1 are comparable with the Dy2−N bond lengths (2.555 and 2.557 Å) in stereoisomer 2, while the mean Dy1−O bond distance(2.336 Å) in stereoisomer 1 is a little longer than the average Dy2−O bond length (2.327 Å) in stereoisomer 2. The shortest Dy···Dy distance in the crystal structure is 9.174 Å, suggesting that intermolecular interactions are negligible.

Table 2. Selected Bond Distances (Å) and Angles (deg) for *d*-1 and *d*-2

		d-**1**	
Dy(1)−O(6)	2.281(6)	Dy(1)−O(2)	2.309(5)
Dy(1)−O(4)	2.328(6)	Dy(1)−O(3)	2.354(6)
Dy(1)−O(5)	2.364(6)	Dy(1)−O(1)	2.378(6)
Dy(1)−N(2)	2.553(7)	Dy(1)−N(1)	2.554(7)
Dy(2)−O(12)	2.276(7)	Dy(2)−O(10)	2.296(6)
Dy(2)−O(8)	2.302(6)	Dy(2)−O(9)	2.345(6)
Dy(2)−O(7)	2.369(5)	Dy(2)−O(11)	2.376(6)
Dy(2)−N(4)	2.555(7)	Dy(2)−N(3)	2.557(7)
N(2)−Dy(1)−N(1)	63.2(2)	N(4)−Dy(2)−N(3)	63.0(2)
O(2)−Dy(1)−O(1)	74.4(2)	O(4)−Dy(1)−O(3)	74.5(2)
O(6)−Dy(1)−O(5)	75.8(2)	O(8)−Dy(2)−O(7)	73.8(2)
O(10)−Dy(2)−O(9)	74.4(2)	O(12)−Dy(2)−O(11)	74.9(2)
		d-**2**	
Dy(1)−O(6)	2.270(6)	Dy(1)−O(4)	2.285(6)
Dy(1)−O(2)	2.323(5)	Dy(1)−O(5)	2.365(5)
Dy(1)−O(1)	2.375(5)	Dy(1)−O(3)	2.421(6)
Dy(1)−N(1)	2.554(7)	Dy(1)−N(2)	2.565(8)
N(1)−Dy(1)−N(2)	64.3(3)	O(2)−Dy(1)−O(1)	74.1(2)
O(4)−Dy(1)−O(3)	73.7(2)	O(6)−Dy(1)−O(5)	73.6(2)

There also exist two homochiral stereoisomers in *l*-**1**, and two Dy^{3+} ions adopt the same coordination modes as those in *d*-**1** (Figure S2). Complexes *l*-**1** and *d*-**1** are a pair of racemic compounds, and their imaging structures are shown in Figure 2. In *l*-**1**, each Dy^{3+} ion also adopts a distorted square antiprismatic environment, with approximate square planes defined as O1−O2−O4−O3 and N1−N2−O6−O5 for the Dy1 atom, and O7−O8−O11−O12 and O9−O10−N4−N3 for the Dy2 atom. The creased angles of two approximate square faces about the respective diagonals O2−O3 and N2−O5 for the Dy1 atom are 10.2° and 7.9°, and the creased angles about the respective diagonals O7−O11 and N3−O10 for the Dy2 atom are 1.2° and 6.5°. Similar to *d*-**1**, the square antiprism polyhedron of the Dy1 atom is more distorted than that of the Dy2 atom.

Unlike *d*-**1**, no any stereoisomerization was observed in *d*-**2**. As shown in Figure 3, the distorted square-antiprism coordination environment of the Dy^{3+} ion in *d*-**2** is quite similar to that of the stereoisomer 2 in *d*-**1** except for the phen capping ligand instead of the bpy capping ligand (Figure S3). The creased angles of two approximate square planes defined as O4−O3−O6−O5 and N1−N2−O1−O2 about the respective diagonals O3−O5 and O1−N1 are 1.5° and 11.2°. The third trifluoroacetyl group of the *d*-tfc$^-$ ligand in *d*-**2** is arranged *trans* to the other two *cis* trifluoroacetyl groups of the *d*-tfc$^-$ ligands. Both the Dy1−N bond distance (mean value of 2.560 Å) and the N−Dy1−N bond angle (64.3°) are a little larger than the corresponding length and angle (mean values of 2.555 Å and 63.1°, respectively) in *d*-**1**. The mean Dy−O bond distance (2.340 Å) is also a little longer than that of *d*-**1** (2.332 Å), but the O−Dy−O bond angle defined by the *d*-tfc$^-$ ligand and the Dy1 atom (mean value of 73.8°) is slightly smaller than the corresponding O−Dy−O bond angle (mean value of 74.6°) of *d*-**1**. The shortest Dy···Dy distance in the crystal structure is 9.777 Å. Complexes *l*-**2** and *d*-**2** are a pair of racemic compounds, and their imaging structures are shown in Figure 3. The Dy^{3+} ion adopts the same coordination mode as that in *d*-**2** (Figure S4). The creased angles of two approximate square planes defined as O4−O3−O6−O5 and N1−N2−O1−O2 about the respective diagonals O3−O5 and O1−N1 are 0.1° and 13.1°.

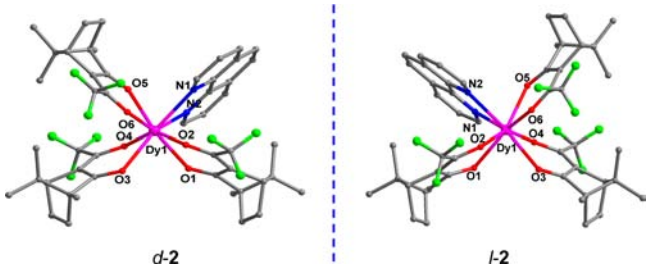

Figure 3. Enantiomeric pair of *d*-**2** and *l*-**2**, and all H atoms and two hydrate molecules of *d*-**2** are omitted for clarity.

Magnetic Properties. Direct-current (dc) magnetic susceptibility studies of *d*-**1**/*l*-**1** and *d*-**2**/*l*-**2** were performed under a field of 1000 Oe in the temperature range 2−300 K. Since the enantiomers possess similar magnetic behaviors, only the magnetic properties of *d*-**1** and *d*-**2** are described in detail. The plots of χT versus T are shown in Figure 4. The χT value at room temperature for *d*-**1** is 28.54 cm^3 K mol^{-1}, in good agreement with the theoretic value of 28.34 cm^3 K mol^{-1} for two uncoupled Dy^{3+} ions ($S = {}^5/_2$, $L = 5$, $^6H_{15/2}$, $g = {}^4/_3$), while the χT value of 14.64 cm^3 K mol^{-1} at 300 K for *d*-**2** is close to the expected value of 14.17 cm^3 K mol^{-1} for the single Dy^{3+} ion. Upon cooling, the χT product of both compounds decreases slowly and remains almost constant and then falls

dx.doi.org/10.1021/ic4011218 | Inorg. Chem. 2013, 52, 8933−8940

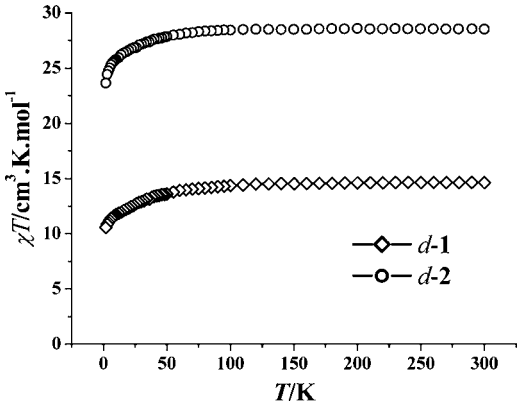

Figure 4. χT versus T plots for *d*-**1** and *d*-**2**.

rapidly when $T < 50$ K, down to minimum values of 23.65 and 10.55 cm^3 K mol^{-1} at 2 K, respectively, which is mostly due to the crystal-field effects (thermal depopulation of the Dy^{3+} Stark sublevels).[14] The magnetization variation for *d*-**1** and *d*-**2** at different applied fields was determined between 2 and 7 K (Figure 5); the nonsuperposition of the isofield lines in the M versus H/T plots suggests the significant anisotropy and/or low-lying excited states of the Dy^{3+} ion in both complexes.

To investigate the spin dynamics, alternating-current (ac) magnetic susceptibilities were measured. When the static field was zero, *d*-**1** exhibits the frequency dependence of magnetic susceptibilities in out-of-phase at low temperature, but no peak was observed (Figure S5). The relaxation of SMMs can be partially influenced by quantum effects, and the application of a dc field probably may remove the ground state degeneracy and induce the quantum tunneling effects.[15] Therefore, the variable temperature ac susceptibility at 250 Hz was measured with application of small dc fields for checking for quantum tunneling effects above 2 K. As shown in Figure S6, the optimum field is 1000 Oe, so ac susceptibility measurements as a function of temperature were determined again under a dc field of 1000 Oe. Now both the χ' and χ'' signals are strongly frequency-dependent below 15 K, and good peak shapes are observed (Figure 6a). Notably, there are two thermally

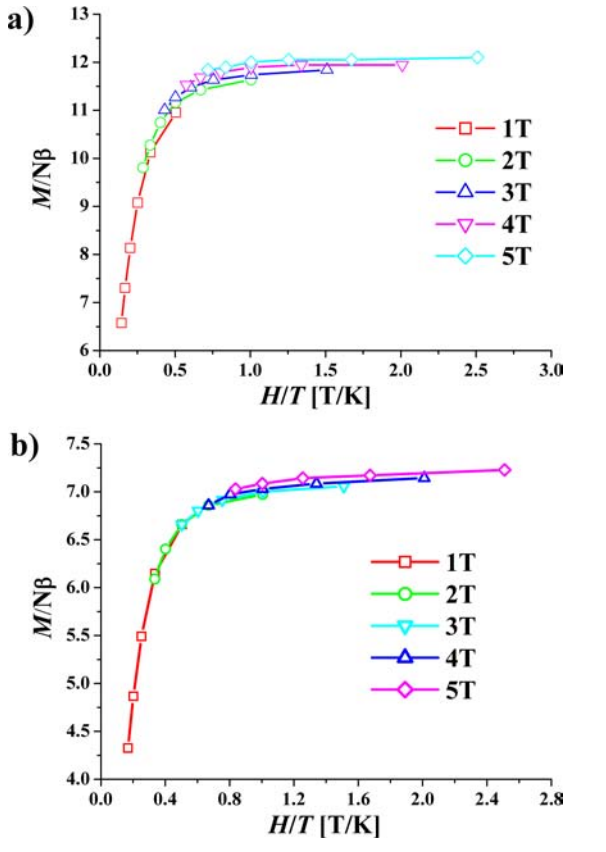

Figure 5. Plots of reduced magnetization ($M/N\beta$) vs H/T for *d*-**1** (a) and *d*-**2** (b).

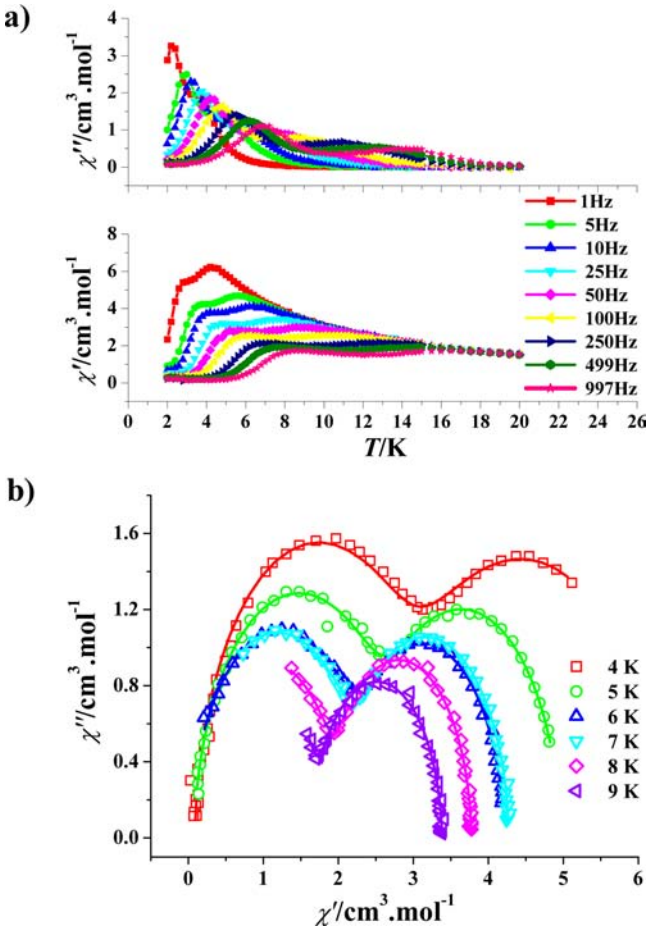

Figure 6. Alternating-current susceptibilities measured in a 2.5 Oe ac magnetic field with a 1 kOe dc-field for *d*-**1** (a) and Cole−Cole plots at 3−9 K for *d*-**1** (H_{dc} = 1 kOe and H_{ac} = 2.5 Oe). The solid lines represent the best fitting with the sum of two modified Debye functions (b).

activated relaxation phases, corresponding to the low-temperature signal region and the high-temperature signal region. The shift of peak temperature (T_f) of χ'' was assessed using the parameter $\phi = (\Delta T_f/T_f)/\Delta(\log f)$ (f denotes the frequency), and gave the value of 0.33, in good agreement with a normal value for a superparamagnet ($\phi > 0.1$) rather than a spin glass state ($\phi \approx 0.01$),[16] confirming the SIM behaviors of *d*-**1**.

To further understand the nature of the two types of dynamics, two sets of magnetization relaxation parameters in the form of $\ln(\tau)$ versus $1/T$ plots were analyzed by the Arrhenius law, $\tau = \tau_0 \exp(U_{eff}/k_B)$, extracting two effective energy barriers, with U_{eff} = 36.5 K ($\tau_0 = 7.9 \times 10^{-7}$ s) and U_{eff} = 46.1 K ($\tau_0 = 6.4 \times 10^{-6}$ s), respectively (Figure S7). These values are consistent with the expected τ_0 values of 10^{-6}−10^{-11}

dx.doi.org/10.1021/ic4011218 | Inorg. Chem. 2013, 52, 8933−8940

s for SMMs/SIMs reported previously. Both thermally activated relaxation processes are ascribed to the Orbach process,[6h] because two τ_0 values are similar, and 36.5 K versus 46.1 K is not much of a difference. The existence of two-step relaxation of the magnetization in *d*-**1** was also supported by the dynamic investigations of magnetic behaviors in the Cole−Cole plots in the form of χ'' versus χ'. The two separate relaxation processes are obviously observed in the semicircle Cole−Cole diagrams at 4−9 K (Figure 6b), which could be well fitted using the sum of two modified Debye models.[17]

$$\chi_{ac}(\omega) = \frac{\chi_2 - \chi_1}{1 + (i\omega\tau_2)^{(1-\alpha_2)}} + \frac{\chi_1 - \chi_0}{1 + (i\omega\tau_1)^{(1-\alpha_1)}} + \chi_0 \quad (1)$$

$$\chi' = \frac{(\chi_2 - \chi_1)[1 + (\omega\tau_2)^{1-\alpha_2}\sin 1/2\alpha_2\pi]}{1 + 2(\omega\tau_2)^{(1-\alpha_2)}\sin 1/2\alpha_2\pi + (\omega\tau_2)^{2(1-\alpha_2)}} + \frac{(\chi_1 - \chi_0)[1 + (\omega\tau_1)^{1-\alpha_1}\sin 1/2\alpha_1\pi]}{1 + 2(\omega\tau_1)^{(1-\alpha_1)}\sin 1/2\alpha_1\pi + (\omega\tau_1)^{2(1-\alpha_1)}} + \chi_0 \quad (2)$$

$$\chi'' = \frac{(\chi_2 - \chi_1)[(\omega\tau_2)^{1-\alpha_2}\cos 1/2\alpha_2\pi]}{1 + 2(\omega\tau_2)^{(1-\alpha_2)}\sin 1/2\alpha_2\pi + (\omega\tau_2)^{2(1-\alpha_2)}} + \frac{(\chi_1 - \chi_0)[(\omega\tau_1)^{1-\alpha_1}\cos 1/2\alpha_1\pi]}{1 + 2(\omega\tau_1)^{(1-\alpha_1)}\sin 1/2\alpha_1\pi + (\omega\tau_1)^{2(1-\alpha_1)}} + \chi_0$$

The results are summarized in Table 3 and shown as Figures S8−S13 and Figure 6b. The parameters α_1 and α_2 in eq 1 are used to evaluate slight deviations of the two thermally activated relaxation processes from the corresponding pure Debye processes. Over the temperature range 4−9 K, both the α_1 and α_2 values are less than 0.093, indicating that both thermally activated relaxation processes have a narrow distribution of relaxation time. In addition, the *M* versus *H* plot of *d*-**1** displays no hysteresis at 1.9 K (Figure S14). The magnetization reaches a maximum value of 11.99 $N\beta$ at 50 kOe, lower than the theoretical value for two Dy^{3+} ions ($2 \times g_J \times J = 2 \times 4/3 \times 15/2 = 20\ N\beta$), implying a much smaller effective spin in *d*-**1**.[6f,18] The magnetic behaviors of *l*-**1** are similar to that of *d*-**1** because they are a pair of enantiomers (Figures S15−S26 and Table S1). The Arrhenius analysis allowed two anisotropy barriers to be extracted, with U_{eff} = 37.0 K ($\tau_0 = 7.7 \times 10^{-7}$ s) and U_{eff} = 49.3 K ($\tau_0 = 4.8 \times 10^{-6}$ s), respectively. These U_{eff} values are slightly larger than the corresponding values of *d*-**1** (U_{eff} = 36.5 and 46.1 K, respectively).

Table 3. Linear Combination of Two Modified Debye Model Fitting Parameters from 4 to 9 K of *d*-1 under 1000 Oe Direct-Current Field

T (K)	χ_2 ($cm^3\ mol^{-1}$)	χ_1 ($cm^3\ mol^{-1}$)	χ_0 ($cm^3\ mol^{-1}$)	τ_1 (s)	α_1	τ_2 (s)	α_2
4	6.38	2.87	0.086 22	0.003 78	0.022	0.108 79	0.093
5	4.98	2.60	0.069 63	0.0012	0.047	0.031 96	0.057
6	4.21	2.25	0.000 06	0.000 42	0.068	0.012 67	0.037
7	4.28	2.21	0.014 35	0.000 16	0.050	0.006 01	0.030
8	3.77	1.94	0.085 03	0.000 07	0.030	0.003 19	0.020
9	3.38	1.72	0.000 02	0.000 03	0.012	0.001 87	0.032

To date, more and more multiple relaxations of magnetization have been observed in SMMs,[6h,11e,f,17b,19] which even can happen in mononuclear Dy^{3+} complexes induced by dilution and/or magnetic field.[19i] Although different mechanisms maybe are involved, the distinction of metal coordination environments has been believed to be one probable cause to take charge of the multiple relaxation of SMMs. For example, Hendrickson et al. postulated that the "Jahn−Teller isomerism" in the $[Mn_{12}O_{12}]$ core is responsible for the second relaxation process of the $[Mn_{12}O_{12}(O_2CR)_{16}(H_2O)_4]$ SMMs;[20] the two thermally activated magnetic relaxation processes of the mononuclear organometallic single-ion magnet $(C_8H_8)Ln(C_5Me_5)$ (Ln^{3+} = Er^{3+} or Ho^{3+}, C_8H_8 = cyclooctatetraenide; C_5Me_5 = pentamethylcyclopentadienide) reported by Gao's group are attributed to the existence of two stable conformers with different cyclooctatetraenide conformations at low temperature.[6h,19g] The Dy^{3+} coordination environments of two $Dy(d\text{-tfc})_3(bpy)$ stereoisomers in *d*-**1**/*l*-**1** show some structural differences as described therein before, so two separate slow magnetic relaxation processes probably happen simultaneously when these two stereoisomers are cocrystallized together, and the two-step relaxation of the magnetization of *d*-**1**/*l*-**1** is expected. In comparison, the You group's recent investigations indicated that two polymorphs of the same Dy^{3+} complex may display distinct slow magnetic relaxation behaviors owing to the different local environments of the Dy^{3+} ion.[18] It is noteworthy that such a two-step magnetic relaxation process is generally attributed to different paramagnetic components of the same molecule or two crystallographically independent Dy^{3+} sites;[6h,11e,f,17b,19] our results suggest that growing stereoisomers' cocrystal maybe is a new way to obtain two-step magnetic relaxation behaviors.

The zero-field ac susceptibility of *d*-**2** also cannot show any out-of-phase peak (Figure S27). However, applying a dc field of 1000 Oe allows us to clearly see peaks in χ'' versus *T* plots (Figure 7a). The ϕ value was calculated to be 0.28, precluding any spin glass state ($\phi \approx 0.01$). The $\ln(\tau)$ versus $1/T$ curve of *d*-**2** (Figure S28) was also fitted to the Arrhenius law, giving the U_{eff} value of 30.5 K and the τ_0 value of 1.1×10^{-7} s. The τ_0 value is in the range of those for previously reported SMMs/SIMs, while the U_{eff} value of *d*-**2** (30.5 K) is obviously smaller than both U_{eff} values of *d*-**1** (36.5 and 46.1 K, respectively). At 3 and 4 K, the Cole−Cole diagrams display two nearly semicircular shapes (Figure 7b), and the least-squares fitting by a Debye model[21] gave α = 0.051 and 0.038 for 3 and 4 K, respectively, indicating the narrow distribution of a single relaxation process.[21b] The *M* versus *H* plot of *d*-**2** displays no hysteresis at 1.9 K (Figure S29). The magnetization reaches a maximum value of 7.23 $N\beta$ at 50 kOe, lower than the theoretical value for one Dy^{3+} ion ($1 \times g_J \times J = 1 \times 4/3 \times 15/2 = 10\ N\beta$), implying a smaller effective spin in *d*-**2**.[6f,18] Again, the magnetic properties of *l*-**2** are similar to those of *d*-**2** because they are a pair of enantiomers (Figures S30−S35). Analysis of the out-of phase ac susceptibility data of *l*-**2** gave U_{eff} = 25.1 K ($\tau_0 = 4.0 \times 10^{-7}$ s), which is somewhat smaller than that of *d*-**2** (30.5 K). As a reference, the classical single relaxation process of *d*-**2** and *l*-**2** corroborates that the two-step relaxation of the magnetization in *d*-**1** and *l*-**1** is associated with the two mononuclear Dy stereoisomers.

dx.doi.org/10.1021/ic4011218 | Inorg. Chem. 2013, 52, 8933−8940

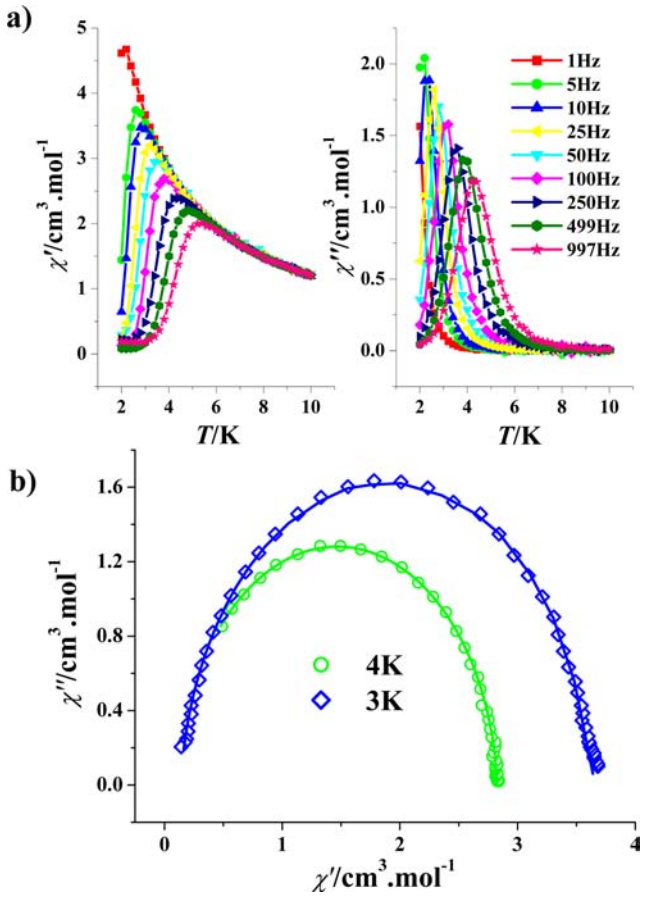

Figure 7. Alternating-current susceptibilities measured in a 2.5 Oe ac magnetic field with a 1 kOe dc field for *d*-**2** (a) and Cole−Cole plots at 3 and 4 K for *d*-**2** (H_{dc} = 1 kOe and H_{ac} = 2.5 Oe); the solid lines represent the best theoretical fitting (b).

CONCLUSIONS

In summary, the enantiopure chiral β-diketonate ligands were successfully applied to construct new homochiral Dy(III) SIMs. The capping diamine ligands have great influence on the structures and magnetic properties of the Dy(III) β-diketonate enantiomeric pairs: when 2,2′-bipyridine acts as the capping ligand, two homochiral Dy(*d*-tfc)$_3$(bpy) or Dy(*l*-tfc)$_3$(bpy) stereoisomers cocrystallize together, exhibiting field-induced SIM behaviors with two separate relaxation processes, while only one homochiral Dy(*d*-tfc)$_3$(phen) or Dy(*l*-tfc)$_3$(phen) conformer and a single relaxation process of the SIM are generated by using 1,10-phenanthroline as the capping ligands. Although isomers of SIMs[18] and single-chain magnets (SCMs)[22] are known, the cocrystal compound *d*-**1**/*l*-**1** represents the first example of a homochiral Dy(III) SIM containing two types of stereoisomers. Furthermore, this work demonstrates that using enantiopure chiral β-diketonate ligands is an effective approach to the assembly of homochiral lanthanide SIMs/SMMs, and growing stereoisomer crystals represents a simple way for modulating SIM/SMM and other physical properties.

ASSOCIATED CONTENT

Supporting Information

X-ray crystallographic data for complexes *d*-**1**, *l*-**1**, *d*-**2**, and *l*-**2** in CIF format. Additional figures of crystal structures (Figures S1−S4) and magnetic characterization (Figures S5−S35 and Table S1). This material is available free of charge via the Internet at http://pubs.acs.org.

AUTHOR INFORMATION

Corresponding Author

*E-mail: cmliu@iccas.ac.cn. Fax: +86-1062559373.

Notes

The authors declare no competing financial interest.

ACKNOWLEDGMENTS

This work was supported by National Key Basic Research Program of China (2013CB933403), National Natural Science Foundation of China (91022014 and 21073198), and Chinese Academy of Sciences.

REFERENCES

(1) (a) Rikken, G. L. J. A.; Raupach, E. *Nature* **1997**, *390*, 493. (b) Rikken, G. L. J. A.; Raupach, E. *Nature* **2000**, *405*, 932. (c) Train, C.; Gheorghe, R.; Krstic, V.; Chamoreau, L.-M.; Ovanesyan, N. S.; Rikken, G. L. J. A.; Gruselle, M.; Verdaguer, M. *Nat. Mater.* **2008**, *7*, 729.

(2) (a) Bogani, L.; Cavigli, L.; Bernot, K.; Sessoli, R.; Gurioli, M.; Gatteschi, D. *J. Mater. Chem.* **2006**, *16*, 2587. (b) Train, C.; Nuida, T.; Gheorghe, R.; Gruselle, M.; Ohkoshi, S.-I. *J. Am. Chem. Soc.* **2009**, *131*, 16838.

(3) (a) Fu, D.-W.; Song, Y.-M.; Wang, G.-X.; Ye, Q.; Xiong, R.-G.; Akutagawa, T.; Nakamura, T.; Chan, P. W. H.; Huang, S. D. *J. Am. Chem. Soc.* **2007**, *129*, 5346. (b) Gu, Z.-G.; Zhou, X.-H.; Jin, Y.-B.; Xiong, R.-G.; Zuo, J.-L.; You, X.-Z. *Inorg. Chem.* **2007**, *46*, 5462. (c) Wang, C.-F.; Li, D.-P.; Chen, X.; Li, X.-M.; Li, Y.-Z.; Zuo, J.-L.; You, X.-Z. *Chem. Commun.* **2009**, 6940. (d) Wen, H.-R.; Tang, Y.-Z.; Liu, C.-M.; Chen, J.-L.; Yu, C.-L. *Inorg. Chem.* **2009**, *48*, 10177. (e) Zhang, W.; Xiong, R.-G. *Chem. Rev.* **2012**, *112*, 1163. (f) Li, X.-L.; Chen, C.-L.; Gao, Y.-L.; Liu, C.-M.; Feng, X.-L.; Gui, Y.-H.; Fang, S.-M. *Dalton Trans.* **2013**, *42*, 5036. (g) Liu, C.-M.; Xiong, R.-G.; Zhang, D.-Q.; Zhu, D.-B. *J. Am. Chem. Soc.* **2010**, *132*, 4044.

(4) Sedó, J.; Ventosa, N.; Ruiz-Molina, D.; Mas, M.; Molins, E.; Rovira, C.; Veciana, J. *Angew. Chem., Int. Ed.* **1998**, *37*, 330. (b) Caneschi, A.; Gatteschi, D.; Rey, P.; Sessoli, R. *Inorg. Chem.* **1991**, *30*, 3936. (c) Kumagai, H.; Inoue, K. *Angew. Chem., Int. Ed.* **1999**, *38*, 1601. (d) Minguet, M.; Luneau, D.; Lhotel, E.; Villar, V.; Paulsen, C.; Amabilino, D. B.; Veciana, J. *Angew. Chem., Int. Ed.* **2002**, *41*, 586. (e) Gao, E. Q.; Yue, Y. F.; Bai, S. Q.; He, Z.; Yan, C. H. *J. Am. Chem. Soc.* **2004**, *126*, 1419. (f) Kaneko, W.; Kitagawa, S.; Ohba, M. *J. Am. Chem. Soc.* **2007**, *129*, 248. (g) Coronado, E.; Gómez-García, C. J.; Nuez, A.; Romero, F. M.; Waerenborgh, J. C. *Chem. Mater.* **2006**, *18*, 2670. (h) Coronado, E.; Galán-Mascarós, J. R.; Gómez-García, C. J.; Murcia-Martínez, A. *Chem.—Eur. J.* **2006**, *12*, 3484. (i) Coronado, E.; Gómez-García, C. J.; Nuez, A.; Romero, F. M.; Rusanov, E.; Stoeckli-Evans, H. *Inorg. Chem.* **2002**, *41*, 4615. (j) Wen, H.-R.; Wang, C.-F.; Li, Y.-Z.; Zuo, J.-L.; Song, Y.; You, X.-Z. *Inorg. Chem.* **2006**, *45*, 7032. (k) Gu, Z.-G.; Song, Y.; Zuo, J.-L.; You, X.-Z. *Inorg. Chem.* **2007**, *46*, 9522. (l) Sereda, O.; Ribas, J.; Stoeckli-Evans, H. *Inorg. Chem.* **2008**, *47*, 5107. (m) Gu, Z.-G.; Xu, Y.-F.; Yin, X.-J.; Zhou, X.-H.; Zuo, J.-L.; You, X.-Z. *Dalton Trans.* **2008**, 5593. (n) Yao, M.-X.; Zheng, Q.; Cai, X.-M.; Li, Y.-Z.; Song, Y.; Zuo, J.-L. *Inorg. Chem.* **2012**, *51*, 2140. (o) Coronado, E.; Dunbar, K. R. *Inorg. Chem.* **2009**, *48*, 3293.

(5) (a) Sessoli, R.; Gatteschi, D.; Caneschi, A.; Novak, M. A. *Nature* **1993**, *365*, 141. (b) Leuenberger, M. N.; Loss, D. *Nature* **2001**, *410*, 789. (c) Wernsdorfer, W.; Aliaga-Alcalde, N.; Hendrickson, D. N.; Christou, G. *Nature* **2002**, *416*, 406. (d) Yamanouchi, M.; Chiba, D.; Matsukura, F.; Ohno, H. *Nature* **2004**, *428*, 539. (e) Bogani, L.; Wernsdorfer, W. *Nat. Mater.* **2008**, *7*, 179. (f) Christou, G.; Gatteschi, D.; Hendrickson, D. N.; Sessoli, R. *MRS Bull.* **2000**, *25*, 66. (g) Benelli, C.; Gatteschi, D. *Chem. Rev.* **2002**, *102*, 2369. (h) Gatteschi, D.; Sessoli, R. *Angew. Chem., Int. Ed.* **2003**, *42*, 268. (i) Aromi, G.; Brechin, E. K. *Struct. Bonding (Berlin)* **2006**, *122*, 1. (j) Coronado, E.; Day, P.

Chem. Rev. **2004**, *104*, 5419. (k) Beltran, L. M. C.; Long, J. R. *Acc. Chem. Res.* **2005**, *38*, 325. (l) Bagai, R.; Christou, G. *Chem. Soc. Rev.* **2009**, *38*, 1011. (m) Chandrasekhar, V.; Murugesapandian, B. *Acc. Chem. Res.* **2009**, *42*, 1047. (n) Sessoli, R.; Powell, A. K. *Coord. Chem. Rew.* **2009**, *253*, 2328. (n) Kostakis, G. E.; Akoab, A. M.; Powell, A. K. *Chem. Soc. Rev.* **2010**, *39*, 2238. (o) Liu, C.-M.; Zhang, D.-Q.; Zhu, D.-B. *Dalton Trans.* **2010**, *39*, 11325. (p) Liu, C.-M.; Zhang, D.-Q.; Hao, X.; Zhu, D.-B. *Cryst. Growth Des.* **2012**, *12*, 2948.

(6) (a) Ishikawa, N.; Sugita, M.; Ishikawa, T.; Koshihara, S.; Kaizu, Y. *J. Am. Chem. Soc.* **2003**, *125*, 8694. (b) Ishikawa, N.; Sugita, M.; Okubo, T.; Tanaka, N.; Iino, T.; Kaizu, Y. *Inorg. Chem.* **2003**, *42*, 2440. (c) AlDamen, M. A.; Clemente-Juan, J. M.; Coronado, E.; Marti-Gastaldo, C.; Gaita-Ariño, A. *J. Am. Chem. Soc.* **2008**, *130*, 8874. (d) Rinehart, J. D.; Long, J. R. *J. Am. Chem. Soc.* **2009**, *131*, 12558. (e) Rinehart, J. D.; Meihaus, K. R.; Long, J. R. *J. Am. Chem. Soc.* **2010**, *132*, 7572. (f) Jiang, S.-D.; Wang, B.-W.; Su, G.; Wang, Z.-M.; Gao, S. *Angew. Chem., Int. Ed.* **2010**, *49*, 7448. (g) Bi, Y.; Guo, Y.-N.; Zhao, L.; Guo, Y.; Lin, S.-Y.; Jiang, S.-D.; Tang, J.-K.; Wang, B.-W.; Gao, S. *Chem.—Eur. J.* **2011**, *17*, 12476. (h) Jiang, S.-D.; Wang, B.-W.; Sun, H.-L.; Wang, Z.-M.; Gao, S. *J. Am. Chem. Soc.* **2011**, *133*, 4730. (i) Cucinotta, G.; Perfetti, M.; Luzon, J.; Etienne, M.; Car, P.-E.; Caneschi, A.; Calvez, G.; Bernot, K.; Sessoli, R. *Angew. Chem., Int. Ed.* **2012**, *51*, 1606. (j) Liu, J.-L.; Yuan, K.; Leng, J.-D.; Ungur, L.; Wernsdorfer, W.; Guo, F.-S.; Chibotaru, L. F.; Tong, M.-L. *Inorg. Chem.* **2012**, *51*, 8538. (k) Chen, G.-J.; Guo, Y.-N.; Tian, J.-L.; Tang, J. k.; Gu, W.; Liu, X.; Yan, S.-P.; Cheng, P.; Liao, D.-Z. *Chem.—Eur. J.* **2012**, *18*, 2484. (l) Ganivet, C. R.; Ballesteros, B.; de la Torre, G.; Clemente-Juan, J. M.; Coronado, E.; Torres, T. *Chem.—Eur. J.* **2013**, *19*, 1457. (m) Menelaou, M.; Ouharrou, F.; Rodríguez, L.; Roubeau, O.; Teat, S. J.; Aliaga-Alcalde, N. *Chem.—Eur. J.* **2012**, *18*, 11545. (n) Wu, S.-Q.; Xie, Q.-W.; An, G.-Y.; Chen, X.; Liu, C.-M.; Cui, A.-L.; Kou, H.-Z. *Dalton Trans.* **2013**, *42*, 4369. (o) Yamashita, A.; Watanabe, A.; Akine, S.; Nabeshima, T.; Nakano, M.; Yamamura, T.; Kajiwara, T. *Angew. Chem., Int. Ed.* **2011**, *50*, 4016.

(7) (a) Rinehart, J. D.; Long, J. R. *J. Am. Chem. Soc.* **2009**, *131*, 12558. (b) Rinehart, J. D.; Meihaus, K. R.; Long, J. R. *J. Am. Chem. Soc.* **2010**, *132*, 7572. (c) Magnani, N.; Apostolidis, C.; Morgenstern, A.; Colineau, E.; Griveau, J.-C.; Bolvin, H.; Walter, O.; Caciuffo, R. *Angew. Chem., Int. Ed.* **2011**, *50*, 1696.

(8) Mossin, S.; Tran, B. L.; Adhikari, D.; Pink, M.; Heinemann, F. W.; Sutter, J.; Szilagyi, R. K.; Meyer, K.; Mindiola, D. J. *J. Am. Chem. Soc.* **2012**, *134*, 13651.

(9) Freedman, D. E.; Harman, W. H.; Harris, T. D.; Long, G. J.; Chang, C. J.; Long, J. R. *J. Am. Chem. Soc.* **2010**, *132*, 1224. (b) Harman, W. H.; Harris, T. D.; Freedman, D. E.; Fong, H.; Chang, A.; Rinehart, J. D.; Ozarowski, A.; Sougrati, M. T.; Grandjean, F.; Long, G. J.; Long, J. R.; Chang, C. J. *J. Am. Chem. Soc.* **2010**, *132*, 18115. (c) Weismann, D.; Sun, Y.; Lan, Y.; Wolmershauser, G.; Powell, A. K.; Sitzmann, H. *Chem.—Eur. J.* **2011**, *17*, 4700. (d) Lin, P.-H.; Smythe, N. C.; Gorelsky, S. I.; Magurire, S.; Henson, N. J.; Korobkov, I.; Scott, B. L.; Gordon, J. C.; Baker, R. T.; Murugesu, M. *J. Am. Chem. Soc.* **2011**, *133*, 15806. (e) Mossin, S.; Tran, B. L.; Adhikari, D.; Pink, M.; Heinemann, F. W.; Sutter, J.; Szilagyi, R. K.; Meyer, K.; Mindiola, D. J. *J. Am. Chem. Soc.* **2012**, *134*, 13651. (f) Zadrozny, J. M.; Atanasov, M.; Bryan, A. M.; Lin, C.-Y.; Rekken, B. D.; Power, P. P.; Neese, F.; Long, J. R. *Chem. Sci.* **2013**, *4*, 125. (g) Atanasov, M.; Zadrozny, J. M.; Long, J. F.; Neese, F. *Chem. Sci.* **2013**, *4*, 139.

(10) (a) Jurca, T.; Farghal, A.; Lin, P.-H.; Korobkov, I.; Murugesu, M.; Richeson, D. S. *J. Am. Chem. Soc.* **2011**, *133*, 15814. (b) Zadrozny, J. M.; Liu, J.; Piro, N. A.; Chang, C. J.; Hill, S.; Long, J. R. *Chem. Commun.* **2012**, *48*, 3927. (c) Vallejo, J.; Castro, I.; Ruiz-García, R.; Cano, J.; Julve, M.; Lloret, F.; De Munno, G.; Wernsdorfer, W.; Pardo, E. *J. Am. Chem. Soc.* **2012**, *134*, 15704. (d) Zadrozny, J. M.; Long, J. R. *J. Am. Chem. Soc.* **2011**, *133*, 20732. (e) Zhu, Y.-Y.; Cui, C.; Zhang, Y.-Q.; Jia, J.-H.; Guo, X.; Gao, C.; Qian, K.; Jiang, S.-D.; Wang, B.-W.; Wang, Z.-M.; Gao, S. *Chem. Sci.* **2013**, *4*, 1802.

(11) (a) Li, D.-P.; Wang, T.-W.; Li, C.-H.; Liu, D.-S.; Li, Y.-Z.; You, X.-Z. *Chem. Commun.* **2010**, *46*, 2929. (b) Zhu, Y.-Y.; Guo, X.; Cui, C.; Wang, B.-W.; Wang, Z.-M.; Gao, S. *Chem. Commun.* **2011**, *47*, 8046. (c) Novitchi, G.; Pilet, G.; Ungur, L.; Moshchalkov, V. V.; Wernsdorfer, W.; Chibotaru, L. F.; Luneau, D.; Powell, A. K. *Chem. Sci.* **2012**, *3*, 1169. (d) Liu, J.; Zhang, X.-P.; Wu, T.; Ma, B.-B.; Wang, T.-W.; Li, C.-H.; Li, Y.-Z.; You, X.-Z. *Inorg. Chem.* **2012**, *51*, 8649. (e) Yao, M.-X.; Zheng, Q.; Gao, F.; Li, Y.-Z.; Song, Y.; Zuo, J.-L. *Dalton Trans.* **2012**, *41*, 13682. (f) Li, X.-L.; Chen, C.-L.; Gao, Y.-L.; Liu, C.-M.; Feng, X.-L.; Gui, Y.-H.; Fang, S.-M. *Chem.—Eur. J.* **2012**, *18*, 14632.

(12) (a) Cunningham, J. A.; Sievers, R. E. *J. Am. Chem. Soc.* **1975**, *97*, 1586. (b) Lennartson, A.; Vestergren, M.; Håkansson, M. *Chem.—Eur. J.* **2005**, *11*, 1757. (c) Lin, Y.; Wan, S.; Zou, F.; Wang, Y.; Zhang, H. *New J. Chem.* **2011**, *35*, 2584. (d) Yuasa, J.; Ohno, T.; Miyata, K.; Tsumatori, H.; Hasegawa, Y.; Kawai, T. *J. Am. Chem. Soc.* **2011**, *133*, 9892.

(13) Drew, M. G. B. *Coord. Chem. Rev.* **1977**, *24*, 179.

(14) Kahn, M. L.; Ballou, R.; Porcher, P.; Kahndagger, O.; Sutter, J.-P. *Chem.—Eur. J.* **2002**, *8*, 525. (b) Kahn, M. L.; Sutter, J.-P.; Golhen, S.; Guionneau, P.; Ouahab, L.; Kahn, O.; Chasseau, D. *J. Am. Chem. Soc.* **2000**, *122*, 3413.

(15) (a) Mishra, A.; Wernsdorfer, W.; Abboud, K. A.; Christou, G. *J. Am. Chem. Soc.* **2004**, *126*, 15648. (b) Moragues-Canovas, M.; Riviere, E.; Ricard, L.; Paulsen, C.; Wernsdorfer, W.; Rajaraman, G.; Brechin, E. K.; Mallah, T. *Adv. Mater.* **2004**, *16*, 1101. (c) Lecren, L.; Wernsdorfer, W.; Li, Y.; Roubeau, O.; Miyasaka, H.; Clérac, R. *J. Am. Chem. Soc.* **2005**, *127*, 11311. (d) Koizumi, S.; Nihei, M.; Shiga, T.; Nakano, M.; Nojiri, H.; Bircher, R.; Waldmann, O.; Ochsenbein, S. T.; Güdel, H. U.; Fernandez-Alonso, F.; Oshio, H. *Chem.—Eur. J.* **2007**, *13*, 8445.

(16) Mydosh, J. A. *Spin Glasses, An Experimental Introduction*; Taylor and Francis: London, 1993.

(17) (a) Grahl, M.; Kotzler, J.; Sessler, I. *J. Magn. Magn. Mater.* **1990**, *90−1*, 187. (b) Guo, Y.-N.; Xu, G.-F.; Gamez, P.; Zhao, L.; Lin, S.-Y.; Deng, R.; Tang, J.; Zhang, H.-J. *J. Am. Chem. Soc.* **2010**, *132*, 8538.

(18) Li, D.-P.; Zhang, X.-P.; Wang, T.-W.; Ma, B.-B.; Li, C.-H.; Li, Y.-Z.; You, X.-Z. *Chem. Commun.* **2011**, *47*, 6867.

(19) (a) Lin, P.-H.; Sun, W.-B.; Yu, M.-F.; Li, G.-M.; Yan, P.-F.; Murugesu, M. *Chem. Commun.* **2011**, *47*, 10993. (b) Langley, S. K.; Chilton, N. F.; Moubaraki, B.; Murray, K. S. *Inorg. Chem.* **2013**, *52*, 7183. (c) Long, J.; Habib, F.; Lin, P.-H.; Korobkov, I.; Enright, G.; Ungur, L.; Wernsdorfer, W.; Chibotaru, L. F.; Murugesu, M. *J. Am. Chem. Soc.* **2011**, *133*, 5319. (d) Wang, Y.-X.; Shi, W.; Li, H.; Song, Y.; Fang, L.; Lan, Y.; Powell, A. K.; Wernsdorfer, W.; Ungur, L.; Chibotaru, L. F.; Shenc, M.; Cheng, P. *Chem. Sci.* **2012**, *3*, 3366. (e) Norel, L.; Bernot, K.; Feng, M.; Roisnel, T.; Caneschi, A.; Sessoli, R.; Rigaut, S. *Chem. Commun.* **2012**, *48*, 3948. (f) Hewitt, I. J.; Tang, J.; Madhu, N. T.; Anson, C. E.; Lan, Y.; Luzon, J.; Etienne, M.; Sessoli, R.; Powell, A. K. *Angew. Chem., Int. Ed.* **2010**, *49*, 6352. (g) Jiang, S.-D.; Liu, S.-S.; Zhou, L.-N.; Wang, B.-W.; Wang, Z.-M.; Gao, S. *Inorg. Chem.* **2012**, *51*, 3079. (h) Leng, J.-D.; Liu, J.-L.; Zheng, Y.-Z.; Ungur, L.; Chibotaru, L. F.; Guo, F.-S.; Tong, M.-L.; Affiliations, S. *Chem. Commun.* **2013**, *49*, 158. (i) Ruiz, J.; Mota, A. J.; Rodríguez-Diéguez, A.; Titos, S.; Herrera, J. M.; Ruiz, E.; Cremades, E.; Costes, J. P.; Colacio, E. *Chem. Commun.* **2012**, *48*, 7916.

(20) Sun, Z.; Ruiz, D.; Dilley, N. R.; Soler, M.; Ribas, J.; Folting, K.; Brian Maple, M.; Christou, G.; Hendrickson, D. N. *Chem. Commun.* **1999**, 1973.

(21) (a) Cole, K. S.; Cole, R. H. *J. Chem. Phys.* **1941**, *9*, 341. (b) Aubin, S. M.; Sun, Z.; Pardi, L.; Krzysteck, J.; Folting, K.; Brunel, L.-J.; Rheingold, A. L.; Christou, G.; Hendrickson, D. N. *Inorg. Chem.* **1999**, *38*, 5329.

(22) Liu, C.-M.; Zhang, D.-Q.; Zhu, D.-B. *Inorg. Chem.* **2009**, *48*, 4980.